Similarities and differences between yeast and vertebrate calmodulin: An examination of the calcium-binding and structural properties of calmodulin from the yeast Saccharomyces cer...

ARTICLE *in* BIOCHEMISTRY · MAY 1993

Impact Factor: 3.02 · DOI: 10.1021/bi00064a008 · Source: PubMed

3 AUTHORS, INCLUDING:

Trisha N Davis
University of Washington Seattle
104 PUBLICATIONS **4,645** CITATIONS

SEE PROFILE

Similarities and Differences between Yeast and Vertebrate Calmodulin: An Examination of the Calcium-Binding and Structural Properties of Calmodulin from the Yeast *Saccharomyces cerevisiae*†

Melissa A. Starovasnik, Trisha N. Davis, and Rachel E. Klevit*

Department of Biochemistry, University of Washington, Seattle, Washington 98195

Received July 28, 1992; Revised Manuscript Received December 29, 1992

ABSTRACT: The Ca^{2+}-binding and structural properties of calmodulin (CaM) from the yeast *Saccharomyces cerevisiae* (yCaM) were analyzed by flow dialysis and NMR spectroscopy. Full-length yCaM and two truncated versions of yCaM were expressed in *Escherichia coli* and purified. yTR1 (residues 1–76) and yTR2 (residues 75–147) are similar to the vertebrate CaM fragments TR1 and TR2, which are generated by limited proteolysis with trypsin. As was found for the fragments of vertebrate CaM, the yCaM fragments retain native conformation and are useful for examining structure and metal-binding properties by NMR. Evidence for a short β-sheet in each domain, as well as characteristic NOEs to aromatic residues, suggests that yCaM folds similarly to vertebrate CaM. Furthermore, although the previously considered "invariant" glycine at position 6 is replaced by a histidine in site II of yCaM, the far downfield chemical shift of His-61's amide proton suggests that this site adopts a conformation similar to that found in other EF-hand sites. Macroscopic Ca^{2+}-binding constants were determined for yCaM by flow dialysis, revealing three high-affinity sites (dissociation constants were 5.2, 3.3, and 2.3 μM in the presence of 1 mM $MgCl_2$ and 100 mM KCl). Positive cooperativity was observed among all sites. Ca^{2+} binding was also monitored indirectly by one-dimensional NMR. Titrations of the fragment molecules reveal that two binding sites reside in the N-terminal domain (sites I and II) and one in the C-terminal domain (site III). All three sites exhibit slow-exchange behavior in the intact protein, but site III exhibits fast-exchange behavior in the isolated C-terminal domain fragment (yTR2). Thus, an interaction between the two domains of intact yCaM affects the behavior of site III. These results with yCaM differ from those of vertebrate CaM in terms of Ca^{2+}-binding stoichiometry, affinity of sites I and II, relative affinity of sites in the N- and C-terminal domains, and the exchange behaviors observed.

Calmodulin (CaM)[1] is a highly conserved ubiquitous Ca^{2+}-binding protein integral to the response to intracellular Ca^{2+} signals [for review see Cohen and Klee (1988)]. The X-ray structure of Ca^{2+}-bound vertebrate CaM (Babu et al., 1988) revealed two similar domains, each with two helix–loop–helix or "EF-hand" Ca^{2+}-binding motifs (Kretsinger & Nockolds, 1973). A similar domain structure was also observed in solution using multidimensional heteronuclear NMR spectroscopy of Ca^{2+}-bound *Drosophila* CaM (Ikura et al., 1991), although the residues linking the two domains exhibited greater flexibility in solution than was apparent in the X-ray structure. Two EF-hand homologs form a structural domain stabilized through a short antiparallel β-sheet and a common hydrophobic core [reviewed in Strynadka and James (1989)]. The residues involved in coordinating Ca^{2+} are found within a contiguous 12-residue sequence that spans the loop and the beginning of the second α-helix. Loop residues 1, 3, 5, and 12 contribute Ca^{2+} ligands through side chain oxygens, and residue 7 ligands through its backbone carbonyl oxygen. An additional ligand is provided by residue 9, either directly through its side chain or indirectly via a water molecule.

The Ca^{2+}-binding and structural properties of CaM from higher eukaryotes have been studied by numerous biophysical methods [reviewed in Forsén et al. (1986)]. All previously studied CaMs (for example, vertebrate, scallop, and *Drosophila*) bind four Ca^{2+}, one in each EF-hand. Spectroscopic studies indicate that these CaMs undergo stepwise Ca^{2+} binding, with sites III and IV having a higher binding affinity than sites I and II (sites are numbered from the N-terminus). The dissociation constants for the four Ca^{2+}-binding sites range from 10^{-6} to 10^{-5} M, and binding to sites III and IV exhibits positive cooperativity [reviewed in Klee (1988)]. Recent reports describing both direct and indirect Ca^{2+}-binding measurements indicate positive cooperativity between sites I and II as well (Klee, 1988; Linse et al., 1991; Starovasnik et al., 1992). Although cooperativity is present within each EF-hand pair, the two globular domains appear to bind Ca^{2+} independently of each other; the Ca^{2+}-binding properties of the domains are indistinguishable whether they are in the intact protein or studied as half-molecule fragments (Drabikowski et al., 1982; Klevit et al., 1984; Ikura et al., 1984; Minowa & Yagi, 1984; Linse et al., 1991).

The Ca^{2+}-binding properties and structural properties of calmodulin from the yeast *Saccharomyces cerevisiae* (yCaM) have not previously been studied in detail. Like CaM from other species, yCaM is heat-stable, acidic, binds Ca^{2+}, shows

† This research was supported by grants to R.E.K. from the National Institutes of Health (DK-35187) and the American Heart Association Established Investigator Award and to T.N.D. from the National Institutes of Health (GM40506) and the Searle Scholars Program/The Chicago Community Trust (88-G-116). M.A.S. was supported by an NSF Predoctoral Fellowship and an NIH Molecular Biophysics Training Grant.

* Author to whom correspondence should be addressed.

[1] Abbreviations: CaM, calmodulin; yCaM, yeast calmodulin; yTR1, yCaM residues 1–76; yTR2, yCaM residues 75–147; TnC, troponin C; NMR, nuclear magnetic resonance; 1D, one dimensional; 2D, two dimensional; NOE, nuclear Overhauser effect; NOESY, NOE spectroscopy; TOCSY, total correlation spectroscopy; CD, circular dichroism; pH*, pH meter reading uncorrected for isotope effects; TSP, sodium 3-(trimethylsilyl)propionate-*2,2,3,3-d*$_4$; EDTA, ethylenediaminetetraacetic acid; EGTA, ethylene glycol bis(β-aminoethyl ether)-*N,N,N',N'*-tetraacetic acid; PMSF, phenylmethanesulfonyl fluoride.

0006-2960/93/0432-3261$04.00/0

FIGURE 1: Amino acid sequence of the Ca^{2+}-binding loops (including the conserved phenylalanine residues) of yCaM (Davis et al., 1986). The one-letter amino acid code is used. The sequence of yCaM (top) is aligned with that of vertebrate CaM (bottom). Only those residues that differ between yeast and vertebrate CaM are shown in the bottom sequence. The 1–12 numbering (above) delineates the 12-residue putative Ca^{2+}-binding loops. Residues predicted to participate in liganding Ca^{2+} are shaded. The one-residue deletion in site IV of yCaM is indicated by the asterisk.

a Ca^{2+}-dependent mobility shift on polyacrylamide gels, and binds to hydrophobic resins in a Ca^{2+}-dependent manner (Davis et al., 1986). yCaM is also rich in α-helical secondary structure as determined by CD spectroscopy (Ohya et al., 1987). Fragments generated by limited proteolysis with trypsin are highly conserved between yeast and vertebrate CaM (Brockerhoff et al., 1992) suggesting a similar tertiary fold. Furthermore, vertebrate CaM can perform the essential function of CaM in yeast (Davis & Thorner, 1989; Ohya & Anraku, 1989; Persechini et al., 1991).

The amino acid sequence of yCaM is 60% identical to that of vertebrate CaM, whereas all known vertebrate CaM sequences are 100% identical (Wylie & Vanaman, 1988). Secondary structure predictions suggest four potential "helix–loop–helix" regions. All four are good matches (at least 14/16) to the EF-hand consensus sequence (Tufty & Kretsinger, 1975). However, yCaM binds only three Ca^{2+} with high affinity (Luan et al., 1987). Notable deviations from the EF-hand consensus occur in sites II and IV. In site II, a histidine replaces the highly conserved glycine (residue 61) at the sixth position of the Ca^{2+}-binding loop (see Figure 1). Site IV is more severely altered; one residue is deleted, and position 12 is a glutamine rather than a glutamate. Glutamate is found at position 12 in all EF-hand sequences known to bind Ca^{2+} (Kretsinger et al., 1991) and provides two of the seven Ca^{2+} ligands (Strynadka & James, 1989). Results from mutational studies (Matsuura et al., 1991) and limited proteolysis (Brockerhoff et al., 1992) suggest that site IV of yCaM is defective in binding Ca^{2+}.

A mutational analysis of yCaM has provided substantial information about the functions of calmodulin in yeast cell growth and division. The phenotypes of a temperature-sensitive yCaM mutant revealed that yCaM is required for proper segregation of the chromosomes during mitosis and is involved in polarized growth and cytokinesis (Davis, 1992). The distribution of yCaM at sites of cell growth throughout the cell cycle also implicates yCaM in the process of cell growth (Brockerhoff & Davis, 1992). Interestingly, mutant yCaMs defective in binding Ca^{2+} support the growth of yeast (Geiser et al., 1991) and have the same cellular distribution as wild-type yCaM (Brockerhoff & Davis, 1992). Thus, the participation of yCaM in mitosis and polarized growth does not depend on its ability to bind Ca^{2+} with high affinity. Nevertheless, yeast does contain both a phosphatase (Cyert et al., 1991; Liu et al., 1991) and a kinase (Miyakawa et al., 1989; Ohya et al., 1991; Pausch et al., 1991) that are activated by yCaM in a Ca^{2+}-dependent manner. The Ca^{2+}–CaM-dependent phosphatase is required during mating (Cyert et al., 1991). Thus, yCaM performs Ca^{2+}-dependent functions during mating as well as the apparently Ca^{2+}-independent functions during mitosis and cell growth.

As a continuation of the mutational analysis of yCaM, over 70 yCaM mutants have been constructed and are being characterized phenotypically (D. van Tuinen, B. H. Chang, J. R. Geiser, and T. N. Davis, unpublished results) However, without detailed structural information about yCaM, we cannot correlate the structural effects of the mutations with the phenotypes that they cause. Although yCaM has many similarities to vertebrate CaM, the two proteins are sufficiently different that they are unlikely to have identical structures. To begin to provide a structural framework within which the mutational analyses can be interpreted, here we report the first detailed analysis of Ca^{2+} binding to yCaM and the first structural analysis of two half-molecule fragments of yCaM. Similar fragments of vertebrate and scallop CaM retain native structural and Ca^{2+}-binding properties and have been useful for dissecting the respective contribution of the individual domains to the overall properties exhibited by CaM (Drabikowski et al., 1982; Andersson et al., 1983; Aulabaugh et al., 1984; Dalgarno et al., 1984; Klevit et al., 1984; Ikura et al., 1984; Minowa & Yagi, 1984; Thulin et al., 1984). When overexpressed in yeast, either the N-terminal or C-terminal half of yCaM can substitute for the full-length protein (Sun et al., 1991). Thus, these truncated forms of yCaM serve not only as model systems to simplify the study of the whole protein but also as distinct functional molecules themselves.

MATERIALS AND METHODS

Strains and Plasmids. All proteins were produced in *Escherichia coli* strain SB1 carrying the plasmid pSB6, which encodes the lysis genes of bacteriophage λ as previously described (Geiser et al., 1991). Plasmid pSB4 (Brockerhoff et al., 1992) was used to produce yCaM. yTR1 was produced from plasmid pMP1 that was derived from pSB4 in two steps. First, the codon encoding Lys-77 was changed to a stop codon by site-directed mutagenesis (Kunkel et al., 1987). Then the portion of CMD1 encoding residues 89–146 was removed by digestion with *Hin*dIII and ligation. yTR2 was produced from plasmid pMN3 constructed as follows. Plasmid pTD30 (Davis et al., 1986) was cut with *Hin*cII and *Sna*B1 to obtain a 335-bp fragment spanning bases 226–561 of CMD1 (+1 is the A of the ATG). A customized *Nco*I linker (GTGCCATG-GCAC) was ligated to the blunt ends. Excess linkers were removed and the fragment was ligated in place of the *Nco*I fragment in pSB4. Plasmid pMN3 encodes a protein Met-Ala-^{75}Gln→^{147}Lys. Electrospray ionization mass spectrometry revealed that the N-terminal Met is uniformly removed from *E. coli*-expressed yCaM, yTR1, and yTR2.

Protein Purification. yCaM was expressed in *E. coli* and purified as described previously using two-step phenyl-Sepharose chromatography (Brockerhoff et al., 1992). Purification of yTR1 and yTR2 was achieved essentially as described for yCaM; however, salt conditions for the second phenyl-Sepharose column differed slightly. Also, an additional purification step by anion-exchange chromatography (DEAE A-25, Pharmacia) was necessary for optimal purity. In all cases protein was applied to phenyl-Sepharose in the presence

of 50 mM Tris, pH 7.5, 10 mM $CaCl_2$, and 1.0 M $(NH_4)_2SO_4$. The column was washed with 10 column volumes of wash buffer consisting of 50 mM Tris, pH 7.5, 5 mM $CaCl_2$, and 0.10 M (yCaM), 0.25 M (yTR1), or 0.40 M (yTR2) $(NH_4)_2SO_4$. Protein was eluted in the presence of 50 mM Tris, pH 7.5, 0.10 M (yCaM and yTR1) or 0.40 M (yTR2) $(NH_4)_2SO_4$, and 50 mM (yCaM and yTR1) or 100 mM (yTR2) EGTA. yTR1 was then dialyzed into 10 mM Tris, pH 7.5, and 1 mM EDTA, loaded onto a DEAE A-25 column equilibrated in the same buffer, and eluted with a linear 0.10–0.80 M NaCl gradient. yTR2 was dialyzed into 10 mM Tris, pH 7.5, and 5 mM $CaCl_2$. The protein was then loaded onto a DEAE A-25 column equilibrated in the same buffer and eluted with a linear 0.0–0.40 M NaCl gradient. yCaM, yTR1, and yTR2 were quantified using estimated extinction coefficients at 257 nm of 1576, 985, and 591 M^{-1} cm^{-1}, respectively (based on the extinction coefficient of phenylalanine multiplied by eight, five, and three phenylalanine residues per molecule; Creighton, 1984). Typical final yields of purified protein were 11 mg (yCaM), 7 mg (yTR1), and 5 mg (yTR2) per liter of cell culture.

NMR samples were made Ca^{2+}-free by addition of 50 mM EGTA and passage over a G-25 desalting column equilibrated in 0.10 M ammonium bicarbonate that had been prepared with water previously run over a Chelex-100 (Bio-Rad) column.

Direct Ca^{2+}-Binding Measurements. Ca^{2+} binding was measured by flow dialysis as described (Maune et al., 1992). Contaminating metals were removed from plasticware, dialysis tubing, and buffers as described (Crouch & Klee, 1980). EGTA was removed from solutions of yCaM by chromatography over two sequential Sephadex G-25 PD-10 columns (Pharmacia-LKB Biotechnology, Inc.) equilibrated in 10 mM Hepes, pH 7.6, 100 mM KCl, and 1 mM $MgSO_4$ (buffer A). yCaM was freed of contaminating metals by passage through a Chelex-100 column (Klee, 1977) equilibrated with buffer A. Levels of Ca^{2+} in samples prepared in buffer A were determined by atomic absorption spectrophotometry (Haiech et al., 1981). The Hill coefficient was obtained by fitting the data to

$$y = \frac{3.0x^n}{K^n + x^n} + jx$$

where y is the number of moles of Ca^{2+} bound per mole of yCaM, x is the concentration of free Ca^{2+}, n is the Hill coefficient, K is the half-saturating concentration of free Ca^{2+}, and j is the slope term for nonspecific binding. Macroscopic Ca^{2+}-binding constants (β_1, β_2, and β_3) were determined by fitting the binding data to the Adair–Klotz equation (Fletcher et al., 1970):

$$y = \frac{\beta_1 x + 2\beta_1\beta_2 x^2 + 3\beta_1\beta_2\beta_3 x^3}{1 + \beta_1 x + \beta_1\beta_2 x^2 + \beta_1\beta_2\beta_3 x^3} + jx$$

where y, x, and j are as defined above. The binding constants were obtained using 29 data points from two experiments. The dissociation constants given in the text (K_1, K_2, and K_3) are simply the reciprocals of the association constants (β_1^{-1}, β_2^{-1}, and β_3^{-1}) determined with the equation above. Binding data obtained at concentrations above 200 μM total Ca^{2+} were not included in the analysis because of nonspecific binding. However, inclusion of all the data (up to 650 μM) would not change the conclusions. The concentration of yCaM was 20.1 μM. Derivative-free nonlinear regression was performed using BMDP statistical software.

NMR Spectroscopy. All NMR spectra were acquired on a Bruker AM-500 spectrometer equipped with a temperature-controlled Haake bath. Typical acquisition parameters for 1D spectra were 6757-Hz spectral width, in 8K points, using a 1.5-s relaxation delay with water presaturation. All NMR samples for Ca^{2+} titrations and temperature studies contained 1.0 mM protein in a total volume of 400 μL containing 50 mM imidazole-d_4, 100 mM KCl, 50 μM EGTA, and 100 μM TSP-d_4, pH* 7.7 in 99.96% D_2O as described (Starovasnik et al., 1992). Samples for 2D NMR spectra contained 2 mM protein prepared either in the same Ca^{2+}-free buffer or with the addition of 10 mM $CaCl_2$. Ca^{2+} titrations were performed by adding 3 μL of a 44 mM stock solution of $CaCl_2$, representing one-third equivalent additions. All titrations were carried out at 25 °C. Titrations were performed at least twice on each sample; a representative experiment is shown. Temperature studies consisted of acquiring 1D spectra over a range of temperatures from 10 to 90 °C in 10 °C increments. Spectra obtained at 25 °C on samples that had been previously heated to 90 °C were identical to those before heat treatment, indicating that the thermal denaturation under study was completely reversible.

Two-dimensional spectra were obtained in the pure-phase absorption mode using time-proportional phase incrementation (Marion & Wüthrich, 1983). Data were processed using the software FTNMR (Hare Research). Two-dimensional data sets were typically 600 × 2K points, processed with sine-bell filters skewed toward $t = 0$, shifted by $\pi/3$ in both dimensions, and zero-filled to produce 1K × 1K matrices. ^1H chemical shifts were referenced to internal TSP. D_2O NOESY spectra shown in Figures 4 and 5 were acquired using a mixing time of 100 ms (yCaM) or 150 ms (yTR1, yTR2) at 30 °C (yCaM) or 25 °C (yTR1 and yTR2). The NOESY spectrum of yTR1 was symmetrized after transformation to remove water ridges for display purposes.

For sequential assignment of yTR1 and yTR2, 2D NOESY and TOCSY spectra were also collected on samples prepared in buffer dissolved in 92% H_2O/8% D_2O. All H_2O NOESY spectra were collected using 150-ms mixing times at pH* 7.4, 25 °C. The water signal was suppressed by saturation between acquisitions and during the NOESY mixing time. The MLEV-17 mixing sequence (Bax & Davis, 1985) was used for TOCSY spectra with mixing times in H_2O of 80 ms (apo-yTR1), 40 ms (Ca^{2+}-yTR1, Ca^{2+}-yTR2), or 75 ms (apo-yTR2); in D_2O TOCSY mixing times used were 80 ms (apo-yTR1), 70 ms (Ca^{2+}-yTR1), and 75 ms (apo-yTR2). In addition, D_2O NOESY (τ_m 150 ms) and TOCSY (τ_m 43 ms) spectra were collected on Ca^{2+}-yTR1 at pH* 8.4, 35 °C to resolve and assign the complete His-61 spin system. Preliminary ^1H NMR assignments (partial assignments for 14 residues of yTR1 and 9 residues of yTR2) are available as supplementary material.

RESULTS

Direct Ca^{2+}-Binding Measurements. Flow dialysis measurements of the binding of Ca^{2+} to yCaM confirmed the existence of three high affinity Ca^{2+}-binding sites (Figure 2A; Luan et al., 1987). Half-maximal binding occurred at 3.4 μM Ca^{2+} and the Hill coefficient of binding was 1.8 with a pseudo r^2 of 0.9998 (Figure 2B and Materials and Methods). The macroscopic binding constants were determined by fitting the data to the Adair–Klotz equation as described in Materials and Methods. The dissociation constants for yCaM are as follows: K_1, 5.2 × 10^{-6} M; K_2, 3.3 × 10^{-6} M; and K_3, 2.3 × 10^{-6} M, with a pseudo r^2 of 0.9997; thus, all three sites have

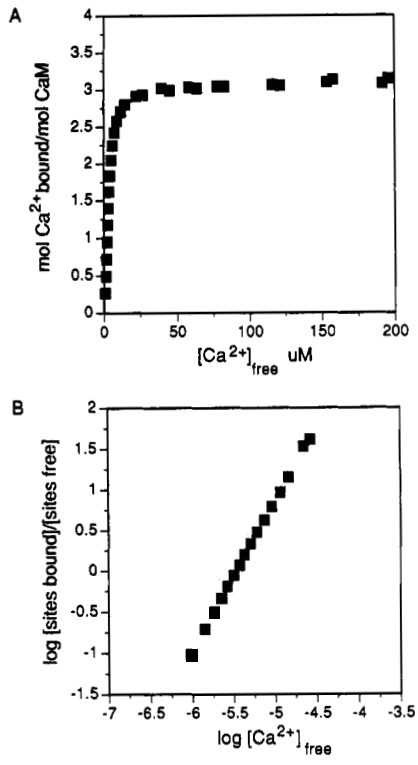

FIGURE 2: Ca^{2+} binding by yCaM. (A) Ca^{2+}-binding data were obtained by flow dialysis as described in Materials and Methods. (B) Hill plot of the Ca^{2+}-binding data for yCaM. Only data obtained at free Ca^{2+} concentrations up to 26 μM were included in this figure.

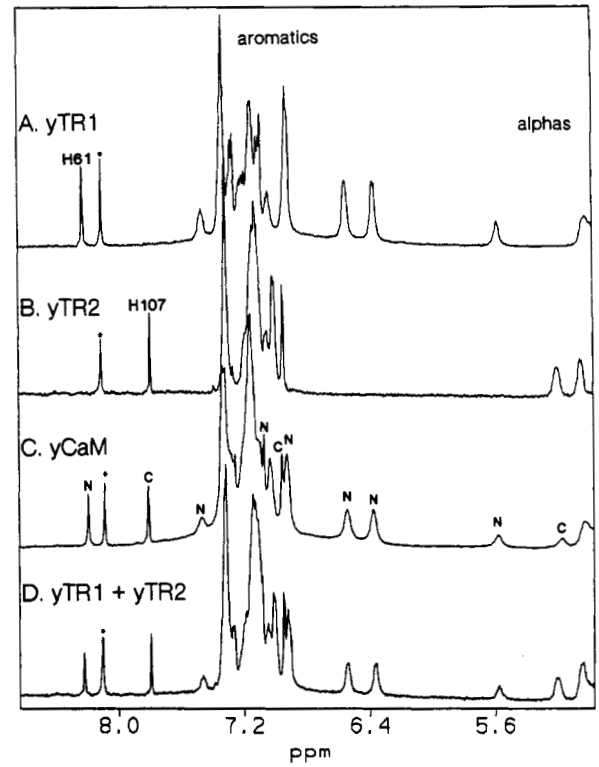

FIGURE 3: Comparison of the 1D NMR spectra of apo yTR1 (A), yTR2 (B), and yCaM (C) at 25 °C. Only the region downfield of water is shown. Spectrum D was generated by adding spectra A and B. The asterisk indicates the residual protonated imidazole buffer peak. Peaks in yCaM that overlap peaks in yTR1 are labeled N to specify that they arise from protons in the N-terminal domain; similarly, peaks in yCaM that overlap peaks in yTR2 are labeled C to specify that they arise from protons in the C-terminal domain.

a similar affinity for Ca^{2+}. The relative values of the three sites ($K_3 < K_2 < K_1$) and the Hill coefficient indicate positive cooperativity among all sites.

Yeast CaM Is Composed of Two Folding Domains. Two approximately half-molecule fragments of yCaM were expressed in *E. coli* and purified to homogeneity. The N-terminal fragment, composed of yCaM residues 1–76, and the C-terminal fragment, composed of residues 75–147, are called yTR1 and yTR2, respectively. These names reflect the relationship to the two fragments that are generated from vertebrate or scallop CaM by limited proteolysis with trypsin in the presence of $CaCl_2$ (Walsh et al., 1977). The downfield regions of the NMR spectra of apo yTR1, yTR2, and yCaM are shown (Figure 3A–C). The spectrum generated by adding the spectra of yTR1 and yTR2 is very similar to that of intact yCaM (compare Figure 3 spectra C and D), suggesting that the two individual domains fold independently into their native structure. The main difference in the spectra is the narrower line width exhibited by the fragment molecules compared with whole yCaM, consistent with their respective molecular sizes. This high degree of chemical shift similarity indicates that resonance assignments obtained from analysis of the spectra of yTR1 and yTR2 will be the same in whole yCaM. As a first stage of resonance assignment, isolated peaks in yCaM were classified as arising from the N- or C-terminal domain, indicated by their presence in the spectrum of yTR1 or yTR2, respectively (see Figure 3).

In order to confirm that yTR1 and yTR2 fold similarly to intact yCaM, 2D ^1H NOESY spectra were examined, portions of which are shown in Figure 4. Peaks in the 2D NOESY spectra of yTR1 and yTR2 are coincident with NOESY peaks in intact yCaM. Examples are the Hα–Hα cross peaks shown in Figure 4 (see arrows). Since NOESY cross peaks arise from interactions between protons that are close in space, matching NOESY patterns indicate retention of native tertiary fold in the fragments. Thus, the similarity of both chemical shift and NOE patterns demonstrates that yTR1 and yTR2 fold independently into their native conformations.

Both Domains of yCaM Structurally Resemble Other EF-Hand Proteins. Because of the high degree of sequence identity and conserved functional properties, the overall folding topology of yCaM is expected to be similar to that of vertebrate CaM and to display structural features common to EF-hand protein domains. A review of the X-ray structures of CaM (Babu et al., 1988), skeletal muscle troponin C (TnC) (Herzberg & James, 1988; Satyshur et al., 1988), parvalbumin (Swain et al., 1989), and intestinal Ca^{2+}-binding protein (Szebenyi & Moffat, 1986; also known as calbindin D_{9k}) reveals that the overall architecture of the structural domain formed by a pair of EF-hand motifs is highly conserved among family members (Strynadka & James, 1989). The two helix–loop–helix motifs interact through a three-residue antiparallel β-sheet involving residues 7–9 from the two 12-residue loops and are related by approximate 2-fold rotational symmetry through the center of the β-sheet. Side chains from all four helices and the two loops interact to form a hydrophobic core. A highly conserved phenylalanine (corresponding to Phe-16 and Phe-89 in the N- and C-terminal domains of CaM, respectively) lies directly over the β-sheet and participates in the hydrophobic core (Figure 5, top).

The NMR spectra of vertebrate and *Drosophila* CaM, parvalbumin, intestinal Ca^{2+}-binding protein, and skeletal and cardiac TnC contain specific indicators of the canonical EF-hand topology described above (Dalgarno et al., 1983a,b, 1984; Seeholzer & Wand, 1989; Kördel et al., 1989; Tsuda et al., 1990; Skelton et al., 1990; Ikura et al., 1991; Brito et al.,

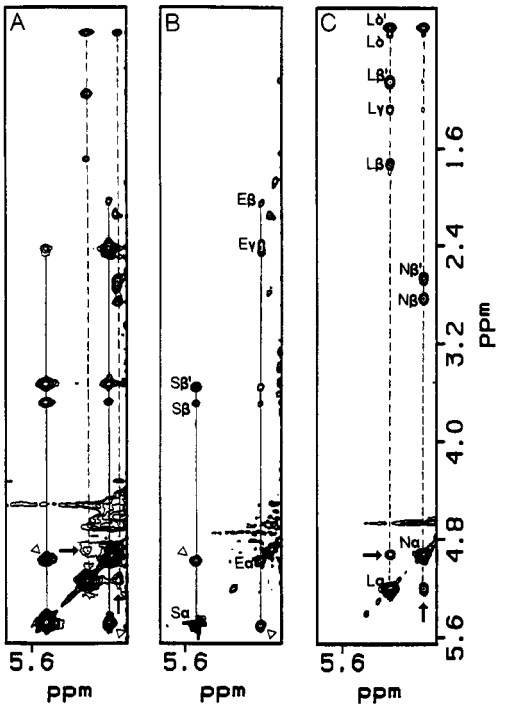

FIGURE 4: Downfield α to aliphatic proton region of the 2D NOESY spectra of apo yCaM (A), yTR1 (B), and yTR2 (C). Spectra were acquired as described in Materials and Methods. Hα–Hα NOEs from the N-terminal domain (triangles) and the C-terminal domain (arrows) of yCaM are indicated. Peaks from the N-terminal domain of yCaM are connected by solid lines; peaks from the C-terminal domain of yCaM are connected by dashed lines. Cross peaks that are also present in the 2D TOCSY spectrum of yTR1 and yTR2 are labeled using the one-letter amino acid code, based on tentative assignments.

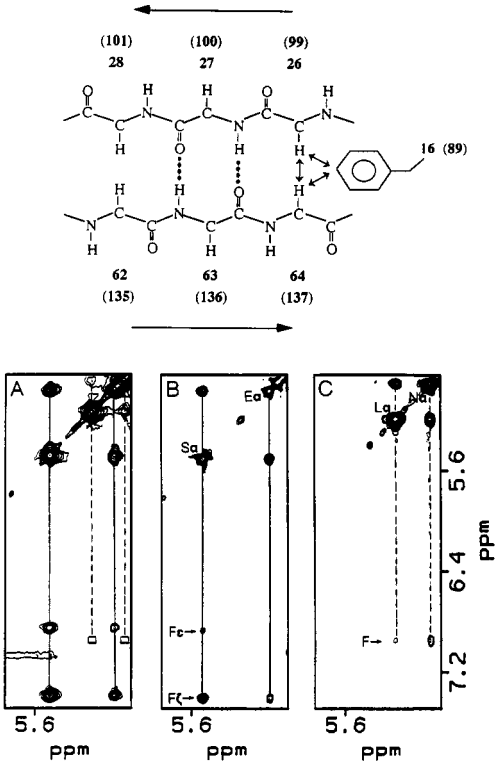

FIGURE 5: (Top) Schematic of the β-sheet of vertebrate CaM that is characteristic of all canonical EF-hand domains. Amino acid residue numbers that participate in forming the β-sheet in the N-terminal domain are as shown; those from the C-terminal domain are included in parentheses. Dotted lines indicate H-bonds found in the X-ray structure of vertebrate CaM (Babu et al., 1988). The phenylalanine residue that lies close to the β-sheet of EF-hand domains is included. NOEs conserved in the NMR spectra of vertebrate CaM, intestinal Ca^{2+}-binding protein, and skeletal and cardiac troponin C are indicated by double-headed arrows. (Bottom) Downfield α to aromatic region of the 2D NOESY spectra of yCaM (A), yTR1 (B), and yTR2 (C). NOEs between protons of Phe-16, Ser-26, and Glu-64 are connected by solid lines. NOEs between protons from a phenylalanine ring, Leu-99, and Asn-137 are connected by dashed lines in yTR2. No corresponding cross peaks are present in this region of yCaM (open boxes) due to the lower signal-to-noise (compare relative intensities of Lα–Nα cross peaks in yCaM and yTR2).

1991). Each exhibits a small number of downfield-shifted Hα peaks, with NOEs observed between these Hα peaks arising from the three-residue antiparallel β-sheet. NOEs are also observed between peaks from a phenylalanine ring and two downfield-shifted Hα peaks. In vertebrate CaM, these NOEs arise from interactions between Phe-16, Thr-26, and Asp-64 in the N-terminal domain and Phe-89, Tyr-99, and Asn-137 in the C-terminal domain (Figure 5, top). These NOEs are observed in both the apo and Ca^{2+}-bound forms of vertebrate and scallop CaM (Dalgarno et al., 1984; Ikura et al., 1985). Observation of analogous NOEs in yCaM would be a strong indication of an analogous tertiary structure.

The NOESY spectra of apo yTR1 and yTR2 contain the following hallmarks of a canonical EF-hand pair fold. In each domain one pair of Hα peaks exhibit NOEs to each other and also to a phenylalanine ring (Figures 4 and 5). The protons that give rise to the most downfield Hα–Hα NOE cross peak in yTR1 have been assigned to Ser-26 and Glu-64 by conventional sequential assignment strategies (Wüthrich, 1986; Englander & Wand, 1987; a table of preliminary ^{1}H resonance assignments is available as supplementary material). In yTR2, the most downfield Hα peak has been sequentially assigned to Leu-99 (Figure 4C). This peak exhibits an NOE to another Hα that, on the basis of analogy with other EF-hands and the fact that the spin system of this peak is consistent with an asparagine residue, is tentatively assigned to Asn-137. All eight phenylalanine residues are conserved between yeast and vertebrate CaM, five in the N-terminal domain and three in the C-terminal domain. In yTR1, there is a phenylalanine ring that gives rise to NOEs with the downfield Hα peaks (Figure 5B) and also gives rise to NOEs with another phenylalanine ring system (not shown), consistent with formation of an "aromatic box" involving Phe-16, Phe-65, and Phe-68 similar to that in the vertebrate CaM structure and conserved in other EF-hand domain structures (Dalgarno et al., 1984; Babu et al., 1988; Strynadka & James, 1989). In apo yTR2 the aromatic resonances are highly overlapped (Figure 3B); however, one phenylalanine clearly exhibits NOEs with the two downfield Hα peaks of yTR2 (Figure 5C). These results are consistent with the β-sheets and overall folds of yTR1 and yTR2 being analogous to those of the N- and C-terminal domains of vertebrate CaM. Therefore, it appears that each domain of yCaM is folded, in general, into the canonical EF-hand pair topology.

Thermal Properties. Further evidence of the structural relatedness of yeast and vertebrate CaM was obtained by examining the thermal denaturation of yCaM, yTR1, and yTR2. The thermal properties of yCaM were measured by analyzing the movement of individual NMR peaks toward their random coil chemical shifts in spectra obtained with increasing temperature. Ca^{2+}-bound yCaM showed little evidence of denaturation even at 90 °C (not shown). In contrast, the ^{1}H NMR spectrum of apo yCaM was much more sensitive to temperature over a range from 10 to 90 °C. The apparent melting temperatures of individual protons in apo yCaM based on the midpoints of their respective

Table I: Thermal Denaturation of apo yCaM, yTR1, and yTR2

Peaks from the N-Terminal Domain			Peaks from the C-Terminal Domain		
	T_m[a] (°C)			T_m[a] (°C)	
resonance	yCaM	yTR1	resonance	yCaM	yTR2
Phe 65 Hδ	55	57–58	Leu-99 Hα	35–45	46–52
Phe 16 Hδ	53	57–58	Met-125 $H_3\epsilon$	44	50
Ser 26 Hα	48–51	55–57	upfield H_3 A	41–45	48–52
Met A $H_3\epsilon$	63	64	upfield H_3 B	37–41	47–51
Met B $H_3\epsilon$	67	65			
Ile 27 $H_3\gamma$	48–50	43–54			
Ile 27 $H_3\delta$	55–58	58–60			
average	56	59		41	49
range	(48–67)	(53–65)		(35–45)	(46–52)
bovine CaM[b]	54	49		36	48

[a] Apparent melting temperature is defined as the temperature at which a given resonance has a chemical shift halfway between the chemical shifts of the native and denatured forms. A range is given for those peaks where there is uncertainty in the midpoint due to resonance overlap. [b] Results from calorimetry studies with apo bovine CaM, TR1, and TR2 (Tsalkova & Privalov, 1985).

temperature-dependent chemical shift perturbations are given in Table I. It is clear from these data that apo yCaM does not unfold in a single cooperative transition. Different peaks migrate toward their random coil chemical shifts with significantly different temperature dependencies, consistent with the existence of two independent folding domains. The N-terminal domain was found to be significantly more stable to thermal denaturation than the C-terminal domain, with an average apparent melting temperature of 56 °C for the former compared to 41 °C for the latter (Table I). The apparent melting temperature of the N-terminal domain was similar whether the domain was isolated in yTR1 or was attached to the C-terminal domain in yCaM. The C-terminal domain, however, denatured at a lower temperature in whole yCaM (~41 °C) than it did when isolated in yTR2 (~49 °C).

Ca^{2+} Titration of yCaM, yTR1, and yTR2 by NMR: (*1*) *Identification of Active Ca^{2+}-Binding Sites.* The Ca^{2+} titration of yCaM monitored by 1D NMR is shown in Figure 6A. As Ca^{2+} is added, the spectrum changes with peaks disappearing and then reappearing at new chemical shift positions. After 3 Ca^{2+} equiv are added, further addition of Ca^{2+} does not affect the spectrum. This result demonstrates that yCaM binds three Ca^{2+} stoichiometrically under the conditions used, in agreement with flow dialysis measurements described above and elsewhere (Luan et al., 1987). Ca^{2+} binding by yTR1 is saturated upon addition of 2 equiv (Figure 6B), indicating that both sites I and II bind Ca^{2+}. In contrast, the Ca^{2+}-induced spectral perturbation of yTR2 is completed upon addition of only 1 Ca^{2+} equiv (Figure 6C), demonstrating that the inactive binding site is in the C-terminal domain.

(*2*) *Relative Order of Ca^{2+} Binding in yCaM.* In vertebrate CaM, the relative order of binding to sites in the N- and C-terminal domains was determined by comparing the midpoints of Ca^{2+}-dependent chemical shift perturbations of specific nuclei with NMR peaks that were sufficiently resolved to be followed throughout a Ca^{2+} titration monitored by 1D NMR (Seamon, 1980; Ikura et al., 1983; Klevit et al., 1984). The difference in the Ca^{2+}-binding affinities between sites located in the N- and C-terminal domains was sufficient to lead to semistepwise binding; peaks from the C-terminal domain titrated in slow exchange and were predominantly affected only during the addition of the first two Ca^{2+} equivalents, whereas peaks from the N-terminal domain titrated in fast exchange and were predominantly affected during the addition of the third and fourth Ca^{2+} equivalents. In contrast, all peaks titrated in slow exchange in yCaM. The only peaks that are resolved throughout the entire Ca^{2+} titration are those from the two histidine rings: the Hε2 resonances from His-61 and His-107 in yCaM were easily assigned by comparison with the single His Hε2 peaks in the spectra of yTR1 and yTR2, respectively (see Figure 3).

The Hε2 peak of His-107 in vertebrate or scallop CaM titrates in concert with other peaks from the C-terminal domain with a transition midpoint near 1.0 mol of Ca^{2+}/mol of CaM (Ikura et al., 1983; Klevit et al., 1984). In contrast, the intensities of the Ca^{2+}-free and Ca^{2+}-bound peaks for His-107 in yCaM are equal when approximately 2.0 Ca^{2+} equiv have been added (see arrow in Figure 6A). Furthermore, whereas peaks from the N-terminal domain of vertebrate and scallop CaM titrate with midpoints near 3.0 mol of Ca^{2+}/mol of CaM (Ikura et al., 1983; Klevit et al., 1984), the Hε2 peak of His-61, in the N-terminal domain of yCaM, undergoes a Ca^{2+}-dependent chemical shift perturbation with a midpoint of approximately 1.3 Ca^{2+} equiv (Figure 6A). These observations suggest that the order of binding to sites in yCaM is not the same as found for vertebrate and scallop CaM. The fact that the N-terminal histidine peak is perturbed at lower Ca^{2+} concentrations than the C-terminal histidine in yCaM suggests that 50% saturation occurs at a lower Ca^{2+} concentration for the N-terminal sites compared with the C-terminal site. Thus, Ca^{2+} appears to bind preferentially to at least one site in the N-terminal domain of yCaM; however, the affinities of sites in the two domains are not very different since His-107 begins shifting before His-61 has finished titrating.

(*3*) *Exchange Behavior.* In both yTR1 and yCaM, Ca^{2+}-binding by sites I and II exhibits slow exchange behavior (i.e., peaks disappear and reappear at new chemical shift positions; see for example His-61 peak in Figure 6A,B). In contrast, the most upfield phenylalanine peaks in the N-terminal domain (tentatively assigned to the Hδ's of Phe-16 and Phe-65) display behavior that differs depending on whether they are in the isolated domain or intact yCaM. In yTR1, these peaks undergo simple slow exchange behavior (Figure 6B). However, in yCaM, the same phenylalanine resonances disappear in slow exchange with added Ca^{2+} but reappear as very broad peaks in the Ca^{2+}-saturated state. This demonstrates that the phenylalanine rings undergo some type of conformational exchange process when yCaM is in its fully Ca^{2+}-bound state that does not occur on the same time scale in the isolated domain. Notice that the His-61 peak (also from the N-terminal domain) does not display this unusual intermediate exchange behavior.

The exchange behavior of site III also depends on whether it is in the context of the truncated or intact protein. In yCaM, site III undergoes slow exchange behavior (see for example His-107 peak in Figure 6A), whereas in yTR2, the domain titrates in fast exchange (i.e., peaks do not disappear and reappear but instead migrate toward their new chemical shift; see for example Asn-137 Hα peak in Figure 6C). Even though the type of exchange behavior exhibited by any individual peak is a function of both the rate of the exchange process being monitored and the magnitude of the chemical shift perturbation induced (Freeman, 1988; Schraml & Bellama, 1988), the aforementioned behavioral difference in the C-terminal domain is indeed attributable to a difference in exchange rates. In yCaM, His-107 undergoes only a very small chemical shift perturbation (~0.1 ppm) yet exhibits slow exchange behavior. In yTR2, however, there are peaks

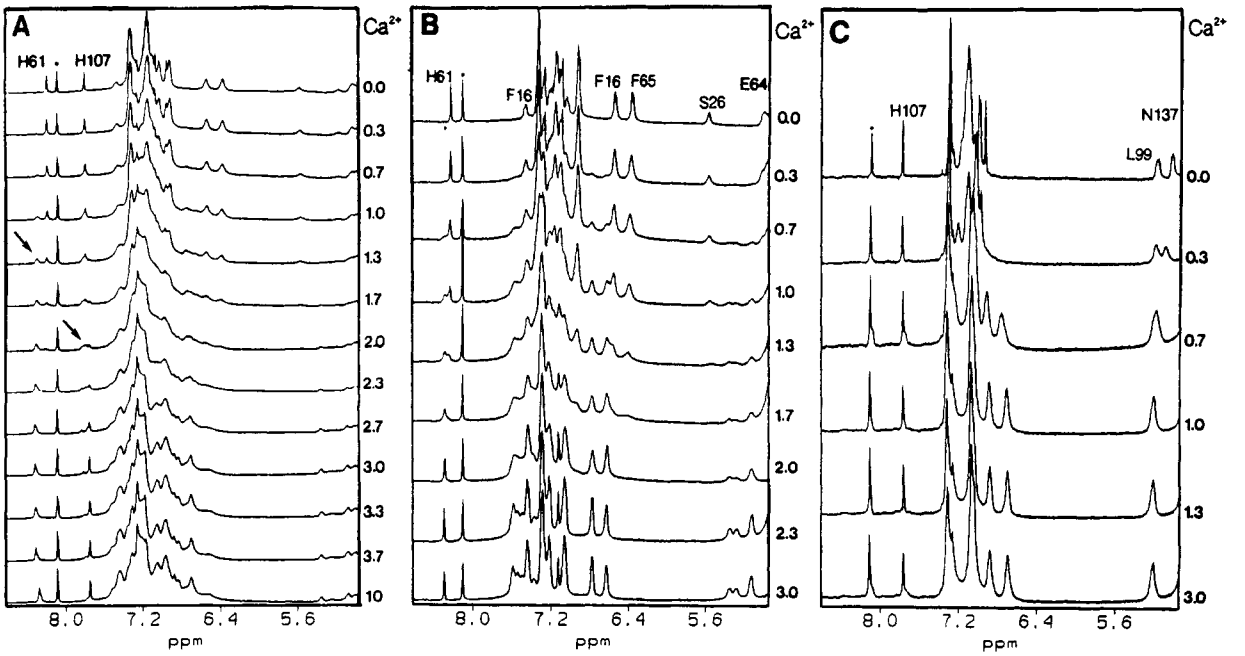

FIGURE 6: Ca^{2+} titration of yCaM (A), yTR1 (B), and yTR2 (C) by NMR. The amount of Ca^{2+} present in a given sample is expressed as moles of Ca^{2+} added per mole of protein. The approximate midpoints of the titrations of His-61 and His-107 in yCaM are indicated by arrows. The asterisk indicates the residual protonanted imidazole buffer peak.

undergoing larger Ca^{2+}-dependent chemical shift changes that exhibit fast exchange behavior (e.g., ~0.2 ppm for Asn-137 Hα, and >0.3 ppm for the most upfield-shifted phenylalanine peak; see Figure 6B). Thus, unlike vertebrate CaM, the exchange behavior of each domain of yCaM depends on whether it exists as an isolated domain or in the context of the whole protein.

(*4*) *Ca^{2+}-Dependent Effects on Downfield-Shifted Amide Proton Resonances.* Amide proton peaks shifted significantly downfield with respect to their random coil positions are found as a characteristic feature of EF-hand Ca^{2+}-binding sites. In *Drosophila* and scallop CaM (Ikura et al., 1987, 1990), skeletal muscle TnC (Tsuda et al., 1988, 1990), cardiac TnC (Krudy et al., 1992), and calbindin D_{9K} (Kördel et al., 1989), the most downfield-shifted peaks in the ^1H NMR spectra (>9.5 ppm) arise from the amide protons of the nearly invariant glycine residues at position 6 from each of the Ca^{2+}-binding loops. In the X-ray structures of EF-hand Ca^{2+}-binding proteins, the amide proton of the position 6 glycine is strongly hydrogen-bonded to one of the side-chain carboxylate oxygens from the highly conserved aspartic acid residue at position 1 of the loop that also serves as one of the Ca^{2+} ligands through its other carboxylate oxygen (Strynadka & James, 1989). In proteins, there appears to be a correlation between chemical shift and hydrogen bonding of amide protons (Pardi et al., 1983; Wishart et al., 1991). Typically, strongly hydrogen-bonded amide protons are found at chemical shifts downfield of their random coil position. Thus, the extreme downfield chemical shifts of the position 6 glycine amide proton resonances observed in solution are consistent with, and perhaps indicative of, formation of hydrogen bonds similar to those observed in the crystal structures of EF-hand proteins.

There are two peaks in Ca^{2+}-free yTR1 and four peaks in Ca^{2+}-bound yTR1 with chemical shifts greater than 9.5 ppm. These peaks have been assigned as shown in Figure 7A. In both the absence and presence of Ca^{2+}, the amide proton of Gly-25 is the most downfield peak in the ^1H NMR spectrum of yTR1, occurring at 10.75 and 10.85 ppm, respectively. Similarly, in Ca^{2+}-bound *Drosophila* CaM, the amide proton of Gly-25 is the most downfield peak from the N-terminal

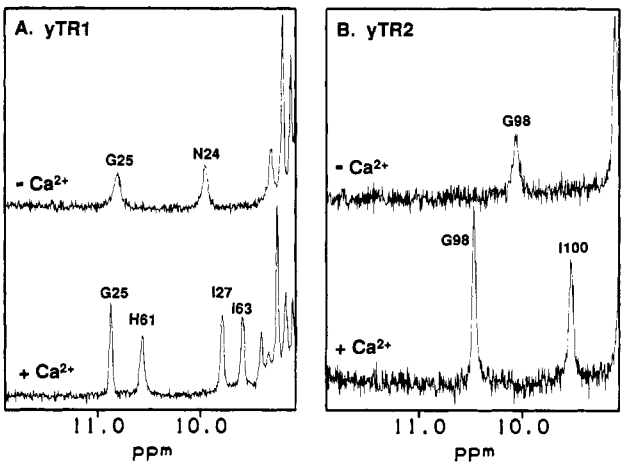

FIGURE 7: Downfield amide proton region of the 1D ^1H NMR spectra of yTR1 (A) and yTR2 (B) in the absence and presence of Ca^{2+}. Spectra shown were obtained on samples containing either 1 mM yTR1 (A) or 0.8 mM yTR2 (B) prepared in buffer containing 50 mM imidazole-d_4, 100 mM NaCl, 50 μM EGTA, and 50 μM TSP, pH 7.4, in 92% H_2O/8% D_2O at 25 °C. The samples used to generate spectra in the presence of Ca^{2+} also contained 2.5 mM (A) or 1.8 mM (B) $CaCl_2$.

domain (Ikura et al., 1990). In yeast and *Drosophila* CaM, site I contains both the conserved aspartic acid (Asp-20) and glycine (Gly-25) residues at Ca^{2+}-binding loop positions 1 and 6, respectively. These similarities suggest that the conformation of the site I Ca^{2+}-binding loop is conserved between yeast and *Drosophila* CaM.

In the presence of Ca^{2+}, the amide proton of His-61 is the second most downfield peak in the yTR1 ^1H NMR spectrum, resonating at 10.55 ppm (Figure 7A). Similarly, in Ca^{2+}-bound *Drosophila* CaM, the amide proton resonance from residue 61 is the second most downfield peak from the N-terminal domain (Ikura et al., 1990). In *Drosophila* CaM, however, residue 61 is the highly conserved position 6 glycine. Site II of yCaM contains the conserved aspartic acid at position 1 (Asp-56), but has a histidine at position 6 (His-61). Although the amide proton resonance for His-61 has not been

specifically assigned in the absence of Ca^{2+}, it clearly does not resonate downfield of 9.5 ppm (see Figure 7A). Therefore, upon Ca^{2+} binding this peak shifts at least 1 ppm downfield. This large shift suggests that His-61 adopts a conformation similar to that observed in a canonical EF-hand loop structure, with the amide proton forming a hydrogen bond with the side-chain carboxylate oxygen of Asp-56, but only when Ca^{2+} is bound.

In apo yTR2, there is only one peak with a chemical shift greater than 9.5 ppm (Figure 7B). This peak (at 10.00 ppm) has been sequentially assigned to the amide proton of the position 6 residue from site III, Gly-98. Upon binding Ca^{2+}, the Gly-98 peak shifts further downfield to 10.46 ppm. The analogous glycine from site IV (Gly-134) is not observed in this region of the spectrum in either the absence or presence of Ca^{2+}. In the C-terminal domain of yCaM, only site III contains both the conserved aspartic acid (Asp-93) and glycine (Gly-98) residues at loop positions 1 and 6, respectively (see Figure 1). Similarly, the N-terminal domain of cardiac TnC contains only one active Ca^{2+}-binding site (Krudy et al., 1992). The inactive site I of cardiac TnC, like site IV of yCaM, lacks the conserved aspartic acid residue at position 1 of the loop and contains glycine at position 6. The behavior observed here for the C-terminal domain of yCaM exactly parallels the pattern of downfield amide proton peaks in the N-terminal domain of cardiac TnC (Krudy et al., 1992). Results from mutation of the site II position 1 aspartic acid residue (Asp-65) in cardiac TnC were consistent with the notion that the downfield shift of the position 6 glycine amide proton is due directly to a hydrogen bond between the backbone amide and the side-chain carboxylate oxygen of the aspartic acid (Krudy et al., 1992).

After the amide peaks from the position 6 residues, the next most downfield peak in Ca^{2+}-yTR1 is from Ile-27; similarly, the next most downfield peak in Ca^{2+}-yTR2 is from Ile-100 (Figure 7). This pattern is identical to that observed in the spectra of Ca^{2+}-bound scallop and *Drosophila* CaM (Ikura et al., 1987, 1990). The amide protons of these residues are involved in cross-strand β-sheet hydrogen bonds in the X-ray structures of vertebrate and *Drosophila* CaM (Babu et al., 1988; Taylor et al., 1991). These data provide further evidence for β-sheet structures in each domain of yCaM similar to those found in other CaM structures.

DISCUSSION

yCaM shares many structural similarities with vertebrate CaM. Both types of CaM are composed of two domains that can fold independently as ~70-residue polypeptides, retaining the tertiary structure inherent in the native protein. Each domain of yCaM has a primary sequence homologous to a pair of EF-hand helix–loop–helix motifs (Kretsinger, 1991; Davis et al., 1986). On the basis of similar NOE patterns observed in the NMR spectra of yeast and vertebrate CaM, it appears that the β-sheet structure conserved in other EF-hand proteins is present in both domains of yCaM. This is perhaps not surprising in the case of the N-terminal domain, which has two active Ca^{2+}-binding sites. However, it is important to note that although the C-terminal domain has a defective Ca^{2+}-binding site, it retains structural features of other EF-hand domains.

The thermal properties of yCaM are very similar to those of vertebrate CaM (Tsalkova & Privalov, 1985). Ca^{2+}-bound yCaM shows little evidence of denaturation even above 90 °C. As is true for other CaMs, the apoprotein has a lower melting temperature than the Ca^{2+}-bound form, and the C-terminal domain has a lower melting temperature than the N-terminal domain. The inherent melting temperature of the Ca^{2+}-free C-terminal domain fragment, yTR2 ($T_m \sim 49$ °C; Table I), is similar to that of vertebrate TR2 (T_m 48 °C; Tsalkova & Privalov, 1985), despite the lack of a functional site IV. In the context of intact yCaM, the C-terminal domain denatures at a lower temperature ($T_m \sim 41$ °C) suggesting a destabilizing interaction exists between the N- and C-terminal domains. A similar destabilization of the C-terminal domain in the intact protein was also detected in vertebrate CaM and rabbit skeletal muscle TnC by calorimetry studies (Tsalkova & Privalov, 1985).

Despite the many similar structural characteristics, the specific Ca^{2+}-binding properties observed for yeast and vertebrate CaMs differ in several respects. First, yCaM binds 3 mol of Ca^{2+}/mol of CaM, whereas vertebrate CaM binds 4 mol of Ca^{2+}/mol of CaM. This difference in Ca^{2+}-binding stoichiometry was not unexpected since the site IV sequence of yCaM lacks key features of an EF-hand Ca^{2+}-binding site (Davis et al., 1986). Second, the macroscopic binding constants are very similar for all three sites in yCaM. Stepwise binding is not observed in the NMR Ca^{2+} titrations; however, there appears to be a slight preference for binding to at least one N-terminal site over the C-terminal site. In contrast, in vertebrate CaM the affinities of the C-terminal sites are 10-fold greater than those of the N-terminal sites, and semi-stepwise binding occurs with the C-terminal sites binding first [reviewed in Forsén et al. (1986)]. Third, binding at all three sites in yCaM shows positive cooperativity. The Hill coefficient is 1.8 and the macroscopic dissociation constants K_2 and K_3 are less than K_1. Positive cooperativity between the N- and C-terminal domains of yCaM is also suggested by the slower exchange behavior of site III in yCaM compared to yTR2. No positive cooperativity between the two domains is evidenced in the results from flow dialysis with vertebrate CaM (Linse et al., 1991). Furthermore, in vertebrate and scallop CaM, Ca^{2+}-binding results obtained with the half-molecule fragments closely mimic results with intact CaM [reviewed in Forsén et al. (1986)].

Sites I and II of yCaM exhibit slow exchange behavior. Since sites I and II of vertebrate CaM exhibit fast exchange behavior (Klevit et al., 1984; Ikura et al., 1984), the slow exchange behavior of sites I and II in yCaM was not anticipated. On the basis of primary sequence comparison with other EF-hand proteins, sites I and II of yCaM would be expected to have binding properties similar to those of sites I and II of vertebrate CaM, except perhaps with reduced affinity due to the replacement of the highly conserved glycine at position 6 in Ca^{2+}-binding loop II with a histidine (see Figure 1). The slower exchange behavior of these sites in yCaM is consistent with the values presented here for the dissociation constants of yCaM as compared to recent results with vertebrate CaM suggesting sites I and II have an approximately 13-fold higher affinity in yCaM than vertebrate CaM. (The dissociation constants of the two lower affinity sites, i.e., sites I and II, of vertebrate CaM are 77×10^{-6} and 14.3×10^{-6} M measured in the presence of 1 mM Mg^{2+} and 100 mM K^+; Klee, 1988.)

What differences are there in sites I and II between yeast and vertebrate CaM that could account for the different Ca^{2+}-binding behaviors? In all EF-hand proteins whose structures have been examined crystallographically, the glycine at position 6 of the loop has ϕ and ψ vaues near 90° and 0°, respectively (Strynadka & James, 1989). Since no other amino acid can readily assume these dihedral angles, prior to these

studies it was thought that the structure of site II in yCaM would differ from other EF-hand proteins to accommodate the histidine while still allowing nearby residues to coordinate Ca^{2+}. However, the chemical shift of the amide proton of His-61, which is similar to that observed for Gly-61 in *Drosophila* CaM, suggests that when Ca^{2+} is bound, a loop conformation is adopted in site II of yCaM similar to that in site II of *Drosophila* CaM. Another notable difference in the sequence of site II of yeast and vertebrate CaM is at position 9. In the X-ray structures of most EF-hand sites, the amino acid at position 9 is a small hydrophilic residue (Ser, Asp, or Asn) that hydrogen-bonds to a water molecule that serves as one of the ligands to the Ca^{2+} (Strynadka & James, 1989). The exception is the CD site of parvalbumin, where there is glutamate at position 9 that ligands the Ca^{2+} directly through one of its side-chain carboxylate oxygens (Swain et al., 1989). In site II of yCaM, there is also a glutamate at position 9 that could potentially ligand the Ca^{2+} directly and may contribute to the higher affinity of sites in the N-terminal domain of yCaM compared with vertebrate CaM.

The most significant conformational differences between yCaM and other CaMs are likely to be found in the C-terminal domain. In vertebrate CaM, the higher affinity of sites in the C-terminal domain can be partly attributed to the presence of positive cooperativity in the binding of sites III and IV (Crouch & Klee, 1980). In yCaM, site III has a high affinity for Ca^{2+} even in the absence of a functional site IV. This is interesting in light of recent results from mutational studies in which the glutamate at position 12 of site IV, Glu-140, was changed to a glutamine or lysine in *Drosophila* CaM (Starovasnik et al., 1992; Maune et al., 1992) or to an alanine in a vertebrate CaM analogue, SYNCAM (Haiech et al., 1991). In these mutant CaMs, disruption of Ca^{2+} binding at site IV is accompanied by a dramatic decrease in Ca^{2+} affinity at the neighboring site III. The high-affinity Ca^{2+} binding exhibited by site III in yCaM suggests that structural differences in the C-terminal domain may compensate for the lack of a functional partner site. The positive interaction between the N- and C-terminal domains of yCaM identified by the different behavior of site III in yTR2 and yCaM may also contribute to the higher affinity of site III in yCaM than would be predicted on the basis of mutagenesis of other CaMs. Future high-resolution structural and mutational analyses will examine which structural features of yCaM are responsible for the unique Ca^{2+}-binding properties of yCaM.

ACKNOWLEDGMENT

We thank Dr. Claude Klee, in whose laboratory the flow dialysis experiments were performed with the expert advice of Dr. Paul Stemmer. We thank Dr. David Teller for help with analysis of the flow dialysis data, Ross Hoffman for many helpful discussions throughout the course of this work, Michael Neff for construction of the yTR2 expression plasmid and development of purification protocols, Adina Ho for purification of yTR2 samples, and Dr. Elinor Adman, Susan Brockerhoff, and Mia Schmiedeskamp for critical reading of the manuscript.

SUPPLEMENTARY MATERIAL AVAILABLE

A table of preliminary ^1H NMR assignments for Ca^{2+}-free and Ca^{2+}-bound yTR1 and yTR2 (2 pages). Ordering information is given on any current masthead page.

REFERENCES

Andersson, A., Forsén, S., Thulin, E., & Vogel, H. J. (1983) *Biochemistry 22*, 2309–2313.

Aulabaugh, A., Niemczura, W. P., & Gibbons, W. A. (1984) *Biochem. Biophys. Res. Commun. 118*, 225–232.

Babu, Y. S., Bugg, C. E., & Cook, W. J. (1988) *J. Mol. Biol. 204*, 191–204.

Bax, A., & Davis, D. G. (1985) *J. Magn. Reson. 65*, 355–360.

Brito, R. M. M., Putkey, J. A., Strynadka, N. C. J., James, M. N. G., & Rosevear, P. R. (1991) *Biochemistry 30*, 10236–10245.

Brockerhoff, S. E., & Davis, T. N. (1992) *J. Cell Biol. 118*, 619–629.

Brockerhoff, S. E., Edmonds, C. G., & Davis, T. N. (1992) *Protein Sci. 1*, 504–516.

Cohen, P., & Klee, C. B., Eds. (1988) *Calmodulin. Molecular Aspects of Cellular Regulation*, Vol. 5, Elsevier, New York.

Creighton, T. E. (1984) *Proteins: Structures and Molecular Properties*, p 17, W. H. Freeman and Co., New York.

Crouch, T. H., & Klee, C. B. (1980) *Biochemistry 19*, 3692–3698.

Cyert, M., Kunisawa, R., Kaim, D., & Thorner, J. (1991) *Proc. Natl. Acad. Sci. U.S.A. 88*, 7376–7380.

Dalgarno, D. C., Levine, B. A., Williams, R. J. P., Fullmer, C. S., & Wasserman, R. H. (1983a) *Eur. J. Biochem. 137*, 523–529.

Dalgarno, D. C., Drabikowski, W., Klevit, R. E., Levine, B. A., Scott, G. M. M., & Williams, R. J. P. (1983b) in *Calcium-Binding Proteins* (de Bernard, B., Sottocassa, G. L., Sandri, G., Carafoli, E., Taylor, A. N., Vanaman, T. C., & Williams, R. J. P., Eds.) pp 83–91, Elsevier, Amsterdam.

Dalgarno, D. C., Klevit, R. E., Levine, B. A., Williams, R. J. P., Dobrowolski, Z., & Drabikowski, W. (1984) *Biochim. Biophys. Acta 791*, 164–172.

Davis, T. N. (1992) *J. Cell Biol. 118*, 607–617.

Davis, T. N., & Thorner, J. (1989) *Proc. Natl. Acad. Sci. U.S.A. 86*, 7909–7913.

Davis, T. N., Urdea, M. S., Masiarz, F. R., & Thorner, J. (1986) *Cell 47*, 423–431.

Drabikowski, W., Brzeska, H., & Venyaminov, S. Y. (1982) *J. Biol. Chem. 257*, 11584–11590.

Englander, S. W., & Wand, A. J. (1987) *Biochemistry 26*, 5953–5958.

Forsén, S., Vogel, H. J., & Drakenberg, T. (1986) in *Calcium & Cell Function* (Cheung, W. Y., Ed.) pp 113–157, Academic Press, New York.

Fletcher, J. E., Spector, A. A., & Ashbrook, J. D. (1970) *Biochemistry 9*, 4580–4587.

Freeman, R. (1988) *A Handbook of Nuclear Magnetic Resonance*, pp 28–32, John Wiley & Sons, New York.

Geiser, J. R., van Tuinen, D., Brockerhoff, S. E., Neff, M. M., & Davis, T. N. (1991) *Cell 65*, 949–959.

Haiech, J., Klee, C. B., & Demaille, J. G. (1981) *Biochemistry 20*, 3890–3897.

Haiech, J., Kilhoffer, M.-C., Lukas, T. J., Craig, T. A., Roberts, D. M., & Watterson, D. M. (1991) *J. Biol. Chem. 266*, 3427–3431.

Herzberg, O., & James, M. N. G. (1988) *J. Mol. Biol. 203*, 761–779.

Ikura, M., Hiraoki, T., Hikichi, K., Mikuni, T., Yazawa, M., & Yagi, K. (1983) *Biochemistry 22*, 2573–2579.

Ikura, M., Hiraoki, T., Hikichi, K., Minowa, O., Yamaguchi, H., Yazawa, M., & Yagi, K. (1984) *Biochemistry 23*, 3124–3128.

Ikura, M., Minowa, O., & Hikichi, K. (1985) *Biochemistry 24*, 4264–4269.

Ikura, M., Minowa, O., Yazawa, M., Yagi, K., & Hikichi, K. (1987) *FEBS Lett. 219*, 17–21.

Ikura, M., Kay, L. E., & Bax, A. (1990) *Biochemistry 29*, 4659–4667.

Ikura, M., Kay, L. E., Krinks, M., & Bax, A. (1991) *Biochemistry 30*, 5498–5504.

Klee, C. B. (1977) *Biochemistry 16*, 1017–1024.

Klee, C. B. (1988) in *Calmodulin. Molecular Aspects of Cellular Regulation* (Cohen, P., & Klee, C. B., Eds.) pp 35–56, Elsevier, New York.
Klevit, R. E., Dalgarno, D. C., Levine, B. A., & Williams, R. J. P. (1984) *Eur. J. Biochem. 139*, 109–114.
Kördel, J., Forsén, S., & Chazin, W. J. (1989) *Biochemistry 28*, 7065–7074.
Kretsinger, R. H., & Nockolds, C. E. (1973) *J. Biol. Chem. 248*, 3313–3326.
Kretsinger, R. H., Tolbert, D., Nakayama, S., & Pearson, W. (1991) in *Novel Calcium Binding Proteins* (Heizmann, C., Ed.) pp 17–38, Springer Verlag, New York.
Krudy, G. A., Brito, R. M. M., Putkey, J. A., & Rosevear, P. R. (1992) *Biochemistry 31*, 1595–1602.
Kunkel, T. A., Roberts, J. D., & Zakour, R. A. (1987) *Methods Enzymol. 154*, 367–382.
Linse, S., Helmersson, A., & Forsén, S. (1991) *J. Biol. Chem. 266*, 8050–8054.
Liu, Y., Ishii, S., Toaki, M., Tsutsumi, H., Ohki, O., Akada, R., Tanaka, K., Tsuchiya, E., Fukui, S., & Miyakawa, T. (1991) *Mol. Gen. Genet. 227*, 52–59.
Luan, Y., Matsuura, I., Yazawa, M., Nakamura, T., & Yagi, K. (1987) *J. Biochem. (Tokyo) 102*, 1531–1537.
Marion, D., & Wüthrich, K. (1983) *Biochem. Biophys. Res. Commun. 113*, 967–974.
Matsuura, I., Ishihara, K., Nakai, Y., Yazawa, M., Toda, H., & Yagi, K. (1991) *J. Biochem. (Tokyo) 109*, 190–197.
Maune, J. F., Klee, C. B., & Beckingham, K. (1992) *J. Biol. Chem. 267*, 5286–5295.
Minowa, O., & Yagi, K. (1984) *J. Biochem. (Tokyo) 96*, 1175–1182.
Miyakawa, T., Oka, Y, Tsuchiya, E., & Fukui, S. (1989) *J. Bacteriol. 171*, 1417–1422.
Ohya, Y., & Anraku, Y. (1989) *Biochem. Biophys. Res. Commun. 158*, 541–547.
Ohya, Y., Uno, I., Ishikawa, T., & Anraku, Y. (1987) *Eur. J. Biochem. 168*, 13–19.
Ohya, Y., Kawasaki, H., Suzuki, K., Londesborough, J., & Anraku, Y. (1991) *J. Biol. Chem. 266*, 12784–12794.
Pardi, A., Wagner, G., & Wüthrich, K. (1983) *Eur. J. Biochem. 137*, 445–454.
Pausch, M. H., Kaim, D., Kunisawa, R., Admon, A., & Thorner, J. (1991) *EMBO J. 10*, 1511–1522.
Persechini, A., Kretsinger, R. H., & Davis, T. N. (1991) *Proc. Natl. Acad. Sci. U.S.A. 88*, 449–452.
Satyshur, K. A., Rao, S. T., Pyzalska, D., Drendel, W., Greaser, M., & Sundaralingam, M. (1988) *J. Biol. Chem. 263*, 1628–1647.
Schraml, J., & Bellama, J. M. (1988) *Two-Dimensional NMR Spectroscopy*, pp 132–135, John Wiley & Sons, New York.
Seamon, K. B. (1980) *Biochemistry 19*, 207–215.
Seeholzer, S. H., & Wand, A. J. (1989) *Biochemistry 28*, 4011–4020.
Skelton, N. J., Forsén, S., & Chazin, W. J. (1990) *Biochemistry 29*, 5752–5761.
Starovasnik, M. A., Su, D.-R., Beckingham, K., & Klevit, R. E. (1992) *Protein Sci. 1*, 245–253.
Strynadka, N. C. J., & James, M. N. G. (1989) *Annu. Rev. Biochem. 58*, 951–998.
Sun, G.-H., Ohya, Y., & Anraku, Y. (1991) *J. Biol. Chem. 266*, 7008–7015.
Swain, A. L., Kretsinger, R. H., & Amma, E. L. (1989) *J. Biol. Chem. 264*, 16620–16628.
Szebenyi, D. M. E., & Moffat, K. (1986) *J. Biol. Chem. 261*, 8761–8777.
Taylor, D. A., Sack, J. S., Maune, J. F., Beckingham, K., & Quiocho, F. A. (1991) *J. Biol. Chem. 266*, 21375–21380.
Thulin, E., Andersson, A., Drakenberg, T., Forsén, S., & Vogel, H. J. (1984) *Biochemistry 23*, 1862–1870.
Tsalkova, T. N., & Privalov, P. L. (1985) *J. Mol. Biol. 181*, 533–544.
Tsuda, S., Hasegawa, Y., Yoshida, M., Yagi, K., & Hikichi, K. (1988) *Biochemistry 27*, 4120–4126.
Tsuda, S., Ogura, K., Hasegawa, Y., Yagi, K., & Hikichi, K. (1990) *Biochemistry 29*, 4951–4958.
Tufty, R. M., & Kretsinger, R. H. (1975) *Science 187*, 167–169.
Walsh, M., Stevens, F. C., Kuznicki, J., & Drabikowski, W. (1977) *J. Biol. Chem. 252*, 7440–7443.
Wishart, D. S., Sykes, B. D., & Richards, F. M. (1991) *J. Mol. Biol. 222*, 311–333.
Wüthrich, K. (1986) *NMR of Proteins and Nucleic Acids*, Wiley, New York.
Wylie, D. C., & Vanaman, T. C. (1988) in *Calmodulin. Molecular Aspects of Cellular Regulation* (Cohen, P., & Klee, C. B., Eds.) pp 1–15, Elsevier, New York.